GIS Odyssey Journal

2026 • Volume 6 • Number 1

https://doi.org/10.57599/gisoj.2026.6.1.103

Nilakshi Mazumdar[1], Kesavan Dharanirajan[2], Manoj Sarmah[3], Vishnu Manoj[4]

# SPATIOTEMPORAL DYNAMICS OF URBAN BUILT-UP EXPANSION AND LAND SURFACE TEMPERATURE IN GUWAHATI MUNICIPAL CORPORATION, ASSAM

**Abstract:** In Guwahati, urban growth has increased over the past ten years, and the thermal imprint within the Guwahati Municipal Corporation (GMC) has evolved over the decade. The change in land surface temperature (LST) regime of GMC between 2013 to 2024 is reshaped by the growth of impervious surfaces. The built-up area increased from 24.33 sq. km in 2013 to 40.12 sq. km in 2024, representing about a 65% expansion. The built-up zones were consistently warmer than the non-built-up areas, with the mean LST differences of approximately 1.5-1.98 °C. It shows a consistent urban thermal penalty. The strong and significant within-year NDBI-LST correlations (r = 0.68-0.74) demonstrated that denser impervious cover is a reliable predictor of high surface temperatures. Conversely, relationships between the variations in NDBI and the variations in LST were weak to moderate (r = 0.26-0.31). The results indicate that a thermal difference exists between non-urban and urban surfaces in Guwahati. Although the areal coverage of the thermally stressed built-up land is still growing with the ongoing urbanisation.

**Keywords:** Land Surface Temperature, NDBI, LST, Landsat 8, Google Earth Engine, Built-Up Expansion, Guwahati

Received: 7 May 2026; accepted: 21 May 2026; revised: 23 May 2026



[1]Pondicherry University, Department of Coastal Disaster Management, Sri Vijaya Puram, Andaman & Nicobar Island, India, ORCID ID: https://orcid.org/0009-0007-6562-0912, email: nilakshimazumdar22@gmail.com

[2]Pondicherry University, Department of Coastal Disaster Management, Sri Vijaya Puram, Andaman & Nicobar Island, India, ORCID ID: https://orcid.org/0000-0003-1750-9893, email: dharanirajan@gmail.com

[3] Pondicherry University, Department of Coastal Disaster Management, Sri Vijaya Puram, Andaman & Nicobar Island, India, ORCID ID: https://orcid.org/0009-0009-5799-6594, email: manojsarmah1502@gmail.com

[4] Pondicherry University, Department of Coastal Disaster Management, Sri Vijaya Puram, Andaman & Nicobar Island, India, ORCID ID: https://orcid.org/0009-0002-5414-6243, email: vishnumanoj007@gmail.com

## Introduction

Urban expansion is one of the most apparent and significant changes on Earth's surface in the twenty-first century. As cities grow, it's increasingly substituting the natural landscape, like forests, wetlands, grasslands, and agricultural fields, with hard impervious surfaces, including concrete roads, rooftop structures and paved plazas. Unlike natural land cover, anthropogenic materials have unique thermodynamic profiles that fundamentally change the local energy balance. During the day, they are effective absorbers of shortwave solar energy and store thermal energy within their high-density mass before slowly giving it up as longwave radiation at night. The Urban Heat Island (UHI) effect is a phenomenon that is rooted in this mechanism, wherein the phenomenon of high ambient and surface temperatures exists within the confines of concentrated metropolitan areas as opposed to rural areas (Oke, 1982; Voogt & Oke, 2003). In the past three decades, the thermal impacts of urbanization have shifted to the centre of the scientific debate to be transformed into a burning concern of the environmental regulation and the health of citizens. The growing urban heat causes the growth of physiological distress, the increase of energy loads of indoor cooling, as well as the disruption of local hydrological cycles (Arnfield, 2003; Santamouris, 2020). Therefore, mapping the pace and extent of urbanization is essential in informing evidence-based planning and supporting the development of climate-resilient cities.

Satellite remote sensing has emerged as the most practical and widely adopted tool for monitoring land surface temperature (LST) across large and heterogeneous urban landscapes (Gorelick et al., 2017; Weng et al., 2004). Ground-based meteorological stations, while precise, are sparse and rarely capture the fine-scale spatial variability of surface temperatures within a city. Thermal infrared sensors aboard Landsat satellites, by contrast, can map LST at 30 m spatial resolution across entire urban agglomerations in a single overpass, enabling systematic analysis of intra-urban thermal patterns and their temporal evolution. Among the spectral indices developed to characterise the extent and intensity of built-up surfaces, the Normalised Difference Built-up Index (NDBI) has gained particular traction (Zha et al., 2003). Derived from the shortwave infrared and near-infrared bands of Landsat imagery, NDBI exploits the spectral contrast between impervious surfaces, which reflect strongly in the shortwave infrared and vegetated land, which absorbs in the same wavelengths while reflecting in the near-infrared. The output is a per-pixel continuous measure of built-up intensity that has a positive correlation with LST and can also be thresholded to produce binary built-up classifications. Studies across Indian cities, including Hyderabad, Chennai, Kolkata, and Ahmedabad, have consistently revealed significant positive correlations between NDBI and LST, reinforcing the utility of this index as a diagnostic tool for urban thermal analysis (Guha et al., 2018; Sultana & Satyanarayana, 2020).

In the northeast Indian context, it remains comparatively underrepresented in the LST and urban expansion literature. It is a significant gap, because a number of cities in the region are experiencing a rapid demographic growth due to in-migration, expanding road and rail connectivity, and increased commercial activity associated with improved

connectivity between northeast India and Southeast Asia. The region's main metropolitan centre, Guwahati, is an example of such dynamics with particular intensity. Over the past two decades, dramatic population growth and physical expansion of the city have occurred (Bhattacharjee et al., 2022; Nath et al., 2021), yet studies examining the thermal consequences of this growth at a multi-temporal scale within its formal administrative boundary remain limited, a distinction that distinguishes Guwahati from many other rapidly urbanising Indian cities (Borbora & Das, 2014).

The analytical unit of this study is the Guwahati Municipal Corporation (GMC), which comprises both the formal governance and the spatial boundary of the core urban agglomeration of the city. The time frame 2013-2024 represents a period of especially vigorous built-up development in GMC, bracketing more than a decade of infrastructure investment, housing expansion, and commercial development. Examining this period through three Landsat 8 acquisition windows, 2013, 2018, and 2024, allows both the structural spatial relationship between built-up cover and LST and its temporal evolution to be assessed. The temporal framing also permits a methodologically important distinction to be drawn between within-year correlations, which establish whether hot places are also built-up places in any given year, and change-period correlations, which test the more demanding question of whether the places that experienced built-up growth are specifically the places that warmed, a distinction that has significant implications for causal interpretation (Deilami et al., 2018).

Against this backdrop, the present study was designed with four specific objectives: (i) to quantify the spatial extent of built-up area expansion within the GMC boundary between 2013 and 2024 using NDBI-derived classification from Landsat 8 imagery processed in Google Earth Engine; (ii) to examine whether LST is consistently and significantly higher in built-up areas than in non-built-up areas across all three study years through zonal statistical comparison; (iii) to measure the strength and statistical significance of the pixel-level association between LST and NDBI in each study year and across temporal change periods using Pearson correlation analysis; and (iv) to assess whether the thermal penalty associated with urban built-up surfaces has intensified, moderated, or remained stable over the eleven-year study period, and to interpret what that trajectory implies for the urban thermal environment of Guwahati as its built-up footprint continues to expand.

## Material and methods

**Study area.** The Guwahati Municipal Corporation constitutes the spatial extent for this analysis. GMC includes the central urban agglomeration of Guwahati in the Kamrup Metropolitan district, Assam (Figure *1*). The city is located on the southern bank of the Brahmaputra River, at approximately 25°59'33'' to 26°15'50'' N and 91°10'41'' to 91°33'18'' E. The elevation within the GMC boundary ranges from near river level to over 200 m on the surrounding hill terrain, adding topographic variation that also influences surface temperatures.

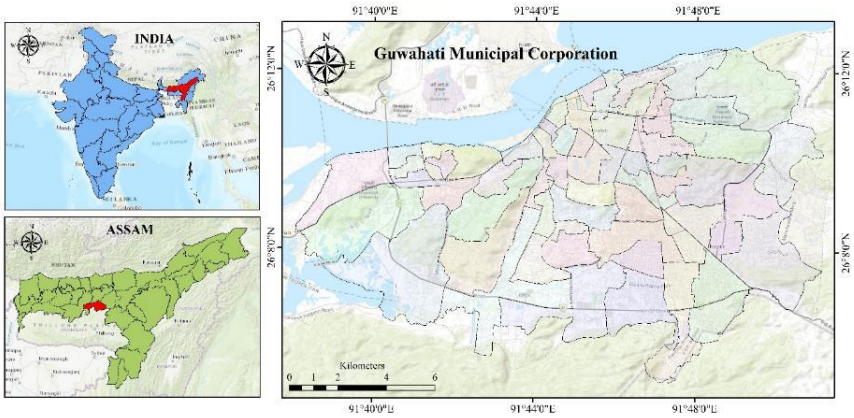


Figure 1. Study area map

Source: Authors' own elaboration based on Survey of India (SOI) topographic maps

The land cover composition of GMC is heterogeneous. Densely built-up fabric occupies the core of the city and extends out in the main road corridors. The foothills of the Shillong Plateau on the southern border, and the north and northeast have wetlands and low-lying floodplain areas. The combination of impervious, vegetated, and water surfaces results in high intra-urban LST gradients, making GMC an effective study site for examining the thermal consequences of urban expansion (Choudhury et al., 2023).

Assam is climatically a humid subtropical to tropical regime with an active monsoon season between June and September. Rainfall is substantial, typically exceeding 1,500 mm annually in Guwahati. The post-monsoon months of November and December, on which the selection of the acquisition window for this study was based, offer relatively low cloud cover and stable atmospheric conditions, making them well-suited to optical and thermal remote sensing.

**Satellite data and image compositing.** Landsat 8 OLI/TIRS Collection 2 Tier 1 Level-2 imagery was accessed through the Google Earth Engine (GEE) JavaScript API (Gorelick et al., 2017). This product provides surface reflectance for the optical bands and land surface temperature for the thermal band in digital number format, with USGS-defined scale factors used in processing. Three acquisition windows were set, with each being November 1 to December 31 of the respective study year. The decision to use the same seasonal window for all three years was deliberate: conditions in late-November and December in Assam are post-monsoon, with lower atmospheric water vapour and a more stable boundary layer than during the wet season. This consistency keeps the thermal and optical signal comparable across years (Table 1).

Table 1. Landsat 8 acquisition parameters for each study year

| Year | Acquisition Window | Cloud Cover Threshold/Rational |
|---|---|---|
| **2013** | 1 Nov - 31 Dec | < 30%; baseline period, pre-expansion thermal conditions |
| **2018** | 2 Nov - 31 Dec | < 30%; mid-period snapshot, five years of urban growth |
| **2024** | 3 Nov - 31 Dec | < 30%; end-period, most recent land cover state |

Source: Authors' own compilation; Landsat 8 Collection 2 imagery accessed via GEE

Scenes exceeding 30% cloud cover were excluded from each collection before any pixel-level processing. Residual cloud and cloud shadow contamination were handled at the pixel scale using the QA_PIXEL band, from which bitwise flags for cloud (bit 3) and cloud shadow (bit 4) were extracted and used as masking conditions. The remaining valid pixels within each annual collection were collapsed into a single median composite clipped to the GMC boundary. Median compositing was preferred over mean compositing for its greater robustness against residual noise from thin cloud and haze that survives the bitmask filter (Roy et al., 2014).

Radiometric conversion followed USGS Collection 2 specifications. Surface reflectance values were obtained by applying the scale factor of 0.0000275 and an additive offset of minus 0.2 to the digital numbers in each optical band. The thermal band ST_B10 was converted to brightness temperature in Kelvin using a scale factor of 0.00341802 and an additive offset of 149.0.

**Land surface temperature retrieval**. LST was not taken directly from the calibrated brightness temperature field. An emissivity correction was applied to account for the fact that the sensor captures radiation emitted as a function of both surface temperature and the material-specific radiative efficiency of each pixel (Parastatidis et al., 2017; Sobrino et al., 2004). The correction followed a three-step procedure (Figure 2). First, NDVI was computed from the near-infrared and red bands. From NDVI, proportional vegetation cover (Pv) was estimated using the expression Pv = [(NDVI - 0.2) / (0.5 - 0.2)] squared, clamped between zero and one. The 0.2 and 0.5 thresholds approximate bare soil and full vegetation NDVI values, respectively. Second, land surface emissivity (LSE) was estimated from Pv using the linear mixing model LSE = (0.004 x Pv) + 0.986, which blends vegetation and impervious emissivity fractions at the per-pixel level (Valor, 1996). Third, brightness temperature was corrected using a Planck inversion expression, with the wavelength constant of 10.895 micrometres corresponding to the effective centre wavelength of Landsat 8 Band 10, and the thermal constant rho set to 14380 micrometres Kelvin.

**NDBI derivation and built-up classification**. NDBI was computed from the shortwave infrared and near-infrared bands as NDBI = (SR_B6 - SR_B5) / (SR_B6 + SR_B5) (Zha et al., 2003). Built-up surfaces and compacted bare soil absorb strongly in NIR and reflect more in SWIR relative to vegetated areas, pushing NDBI toward positive values for developed land. NDBI was used in two ways. As a continuous index, it served as a per-pixel measure of built-up surface intensity. As a binary classifier, pixels with NDBI greater than zero were classified as built-up and all others as non-built-up. Built-up area in each year was quantified by multiplying the binary mask by the geodetic pixel area computed from GEE's ee.Image.pixelArea function and summing across the GMC geometry, converting from square metres to square kilometres.

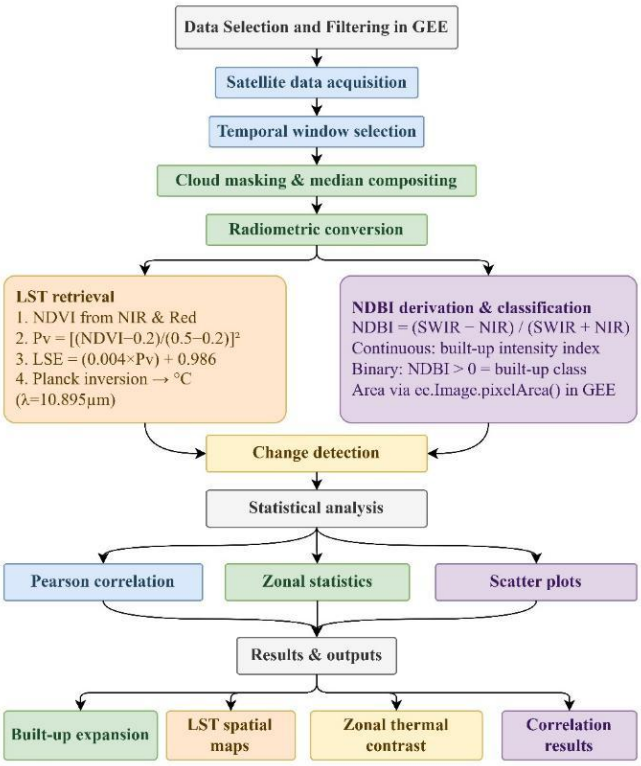


Figure 2. Methodology flow chart
Source: Authors' own elaboration

**Change detection.** Change rasters were produced for three temporal pairs: 2013 to 2018, 2013 to 2024, and 2018 to 2024. For each pair, subtraction rasters were computed for both LST and NDBI. A positive value in the LST change raster means the location warmed over that period. A positive NDBI change indicates increasing built-up intensity. These change rasters were used both for spatial mapping within GEE and as inputs to the change-period correlation analysis.

**Statistical analysis**. Four analytical approaches were applied. Pearson's correlation coefficient was computed between LST and NDBI at the pixel level for each of the three study years and for each of the three change periods, using GEE's built-in Pearson Correlation reducer across all valid pixels at a 30 m scale. A p-value threshold of 0.05 was applied for significance. Correlation strength was interpreted as weak below 0.3, moderate between 0.3 and 0.5, strong between 0.5 and 0.7, and very strong above 0.7. Zonal statistics were computed by masking the LST layer to built-up and non-built-up pixels separately and applying mean reduction within the GMC boundary for each study year. Scatter plots were generated in the GEE console from 500-pixel samples drawn at 90 m resolution with a fixed random seed of 42, each carrying a linear trendline and R-squared display. A 5,000 point random sample at 30 m resolution was exported to Google Drive as a CSV file containing fifteen variables per pixel for supplementary analysis in Microsoft Excel.

## Results

**LST descriptive statistics**. The land surface temperature (LST) showed significant temporal and spatial variability within the Guwahati Municipal Corporation (GMC) during the study period. At the citywide scale, the mean LST was 30.11°C in 2013, declined to 26.06°C in 2018, and subsequently increased to 28.49°C in 2024. A significantly lower set of temperature conditions recorded in November 2018 is probably linked to interannual atmospheric variability during the November-December acquisition period, rather than to the need to record a sustained lowering of urban thermal intensity. The spatial distribution of temperature also became increasingly heterogeneous over time. The standard deviation of LST has increased by 2024 compared to 2013, indicating that the range of thermal conditions across the urban landscape is expanding. This increased heterogeneity is in line with the concurrent expansion of built-up areas and the further fragmentation of vegetated and forested land covers, both of which contribute to uneven patterns of surface heating in the city (Table *2*).

Table 2. Descriptive statistics for LST and LST change across all study periods

| Period | Mean (ºC) | Median (ºC) | Min (ºC) | Max (ºC) | Std Dev |
|---|---|---|---|---|---|
| **LST 2013** | 30.11 | 30.31 | 21.91 | 38.75 | 1.88 |
| **LST 2018** | 26.06 | 26.34 | 19.7 | 32.98 | 1.57 |
| **LST 2024** | 28.49 | 28.69 | 17.64 | 38.85 | 2.21 |
| **LST 2013-2018** | -4.06 | -4.03 | -11.53 | 3.37 | 0.91 |
| **LST 2013-2024** | -1.63 | -1.56 | -11.32 | 6.53 | 1.5 |
| **LST 2018-2024** | 2.43 | 2.44 | -6.73 | 11.8 | 1.62 |

Source: Authors' own elaboration based on Landsat 8 imagery

The LST change rasters can provide more information on temporal changes in urban thermal conditions. The difference image of 2013 and 2018 showed a mean change of -4.06°C, indicating that the 2018 composite was generally colder in the study area. By comparison, the 2018-2024 comparisons showed a mean increase of 2.43ºC, with localised warming of up to 11.8ºC at the pixel level. The net change between the year 2013 and 2024 continued to be negative at 1.63 degree of centigrade, and this was greatly influenced by the relatively low baseline conditions of 1.63 degrees Celsius. Although these changes occur over time, the variability in the change rasters was relatively small. The standard deviation values of 0.91 to 1.62°C indicate that the thermal variation was spatially dispersed rather than clustered in a few isolated hotspots. This trend indicates that the identified thermal changes represent the scale-wide changes in the properties of urban surfaces and the environment in the GMC area. Figure 4 shows four colour-coded maps of the GMC study area that display the Land Surface Temperature (LST) distribution derived from Landsat 8 imagery for 2013, 2018, and 2024, along with an LST change map for 2018–2024. Colours range from green (low

LST) to red (high LST), indicating spatiotemporal variations in urban heat patterns across the study area.

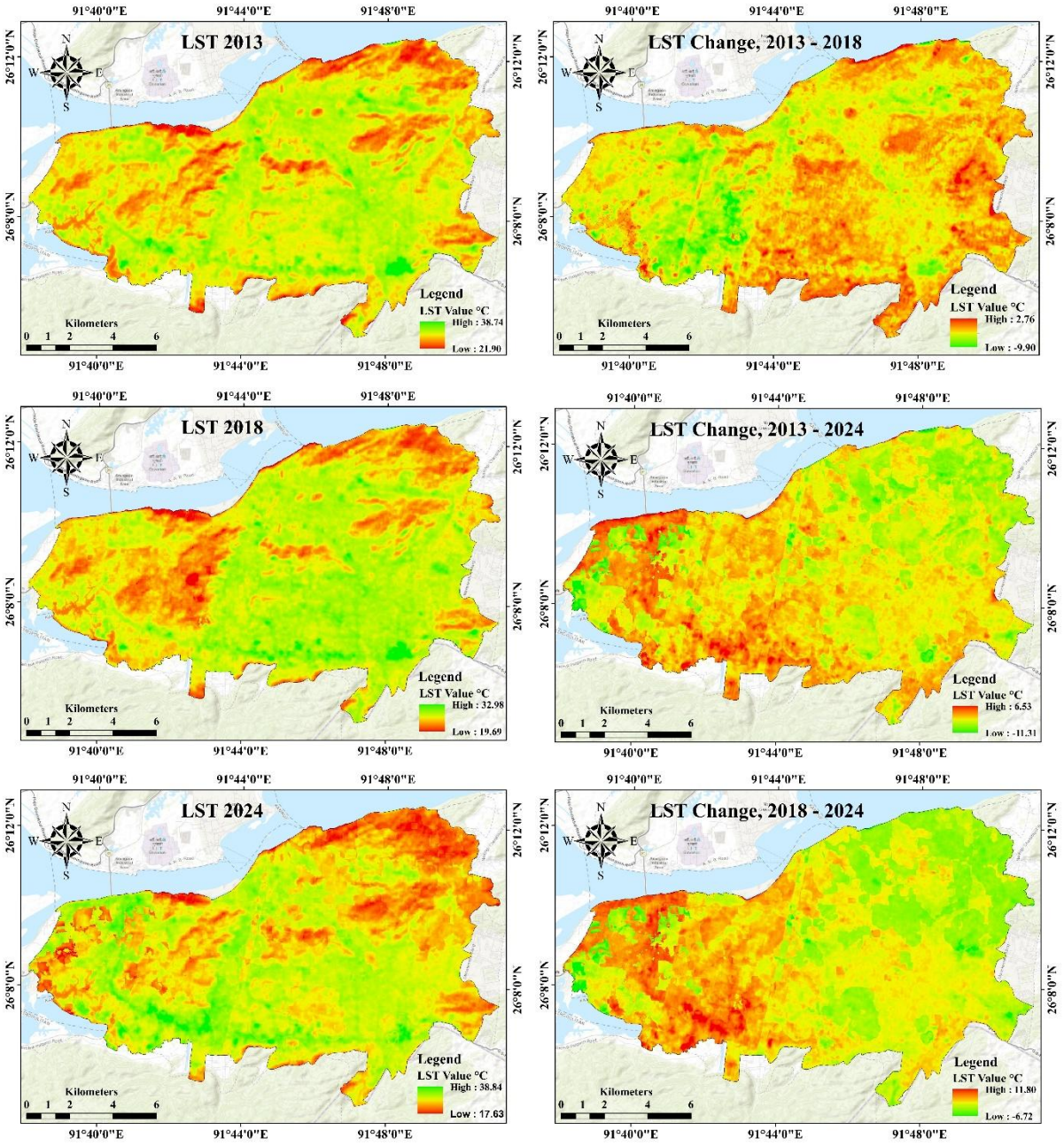


Figure 4. Spatial distribution of LST and its changing pattern across the GMC for 2013, 2018, and 2024
Source: Author's own elaboration based on Landsat 8 imagery

**Built-up area expansion.** The binary built-up classification based on NDBI thresholding indicates continued growth of urban land cover in the GMC study area during the study period. Built-up extent increased from 24.33 sq. km in 2013 to 29.02 sq. km in 2018 and further expanded to 40.12 sq. km by 2024. In total, the net expansion of built-up area in the city was estimated at about 15.79 sq. km between 2013 and 2024, representing a relative expansion of almost 65% over 11 years. The time trend of

expansion suggests that urban expansion was not a steady process. Over the period 2013 to 2018, built-up land increased by approximately 4.69 sq. km per 5 years, whereas the next period, 2018 to 2024, recorded a much higher increase of about 11.10 sq. km per 6 years. This trend implies a further increase in the rate of urban land conversion during the later period of the development, demonstrating increased pressure of urbanisation in the GMC region. Figure 4 presents three colour-coded spatial maps of the GMC study area showing built-up land classification based on the Normalised Difference Built-up Index (NDBI > 0), derived from Landsat 8 imagery for the years 2013, 2018, and 2024. Red and orange tones indicate higher built-up density, while green tones represent lower built-up or vegetated areas, illustrating the spatiotemporal expansion of urban built-up surfaces over the study period.

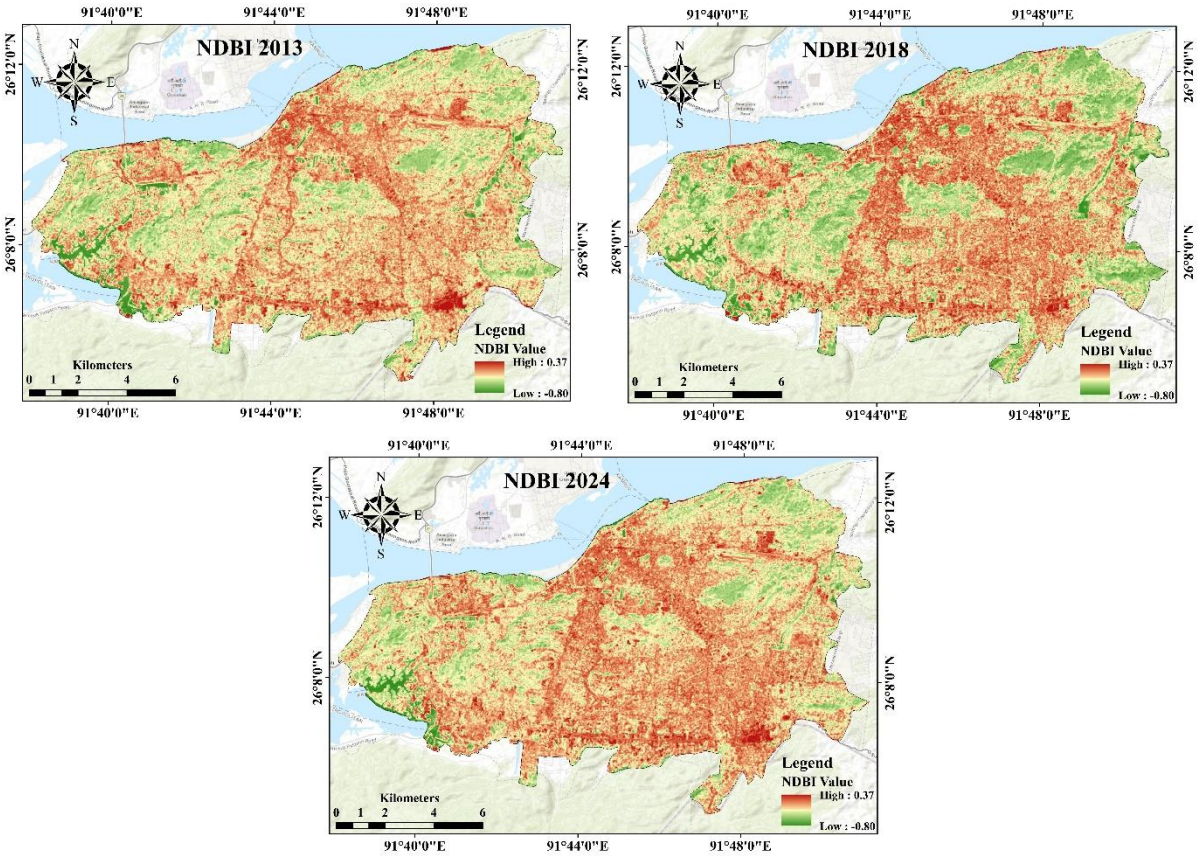


Figure 6. Spatial maps of built-up classification (NDBI > 0) for 2013, 2018, and 2024
Source: Author's own elaboration based on Landsat 8 imagery

**Zonal LST comparison: built-up vs non-built-up.** The mean land surface temperature (LST) was consistently higher in built-up regions than in non-built-up regions throughout the study period, indicating that an urban thermal penalty persisted in the GMC region (Table 3) (Figure 7).

Table 3. Zonal mean LST comparison between built-up and non-built-up areas, with built-up extent for each study year

| Year | Built-up Area (sq. km) | Mean LST Built-up (°C) | Mean LST Non-Built-up (°C) | Diff (°C) |
|---|---|---|---|---|
| **2013** | 24.33 | 31.82 | 29.84 | 1.98 |
| **2018** | 29.02 | 27.31 | 25.81 | 1.5 |
| **2024** | 40.12 | 29.85 | 28.09 | 1.76 |

Source: Authors' own elaboration based on Landsat 8 imagery

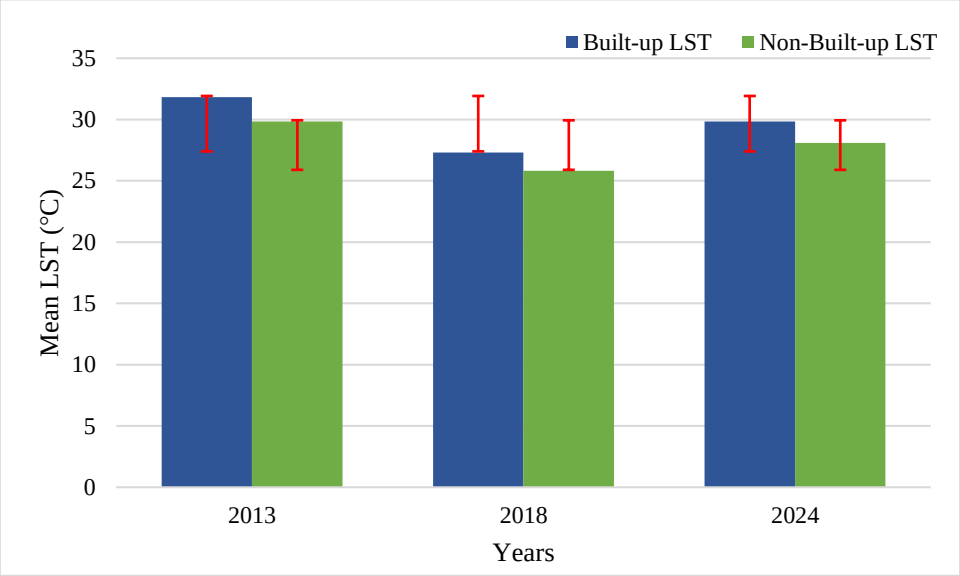


Figure 7. Bar chart comparing mean LST inside and outside built-up areas for 2013, 2018, and 2024, with error bars showing one standard deviation
Source: Authors' own elaboration based on Landsat 8 imagery

In 2013, the built-up surfaces had a mean LST of 31.82°C, compared to 29.84°C in non-built-up areas, resulting in a thermal difference of 1.98°C. Even though the overall temperatures were lower in 2018, consistent with the overall cooler composite conditions, the thermal difference between the two types of land cover remained at 1.76°C. The fact that a positive temperature difference still exists between all three years of observation is an important result of the study. The findings indicate that urbanised surfaces in Guwahati have always recorded higher surface temperatures as compared to non-urban land covers. But more to the point, the main difference between the 2013 and 2024 concerns is not that the thermal contrast itself exists, but that its spatial footprint is growing. With the change in built-up extent, which grew by an average of 65 percent over the study period, an increasingly large share of the city became exposed to the high surface temperatures linked with the change in built-up extent.

**Pearson correlation: LST vs NDBI.** Pearson correlation between land surface temperature (LST) and the Normalised Difference Built-up Index (NDBI) at the pixel level on an annual basis, as well as on the three inter-annual change periods. Table 4, which shows the results, indicates that the relationship between built-up intensity and

surface temperature is always positive and statistically significant throughout the GMC area. The strength of this association, however, indicated that although the thermally distinct surface remained within the urbanised surface, the direct correspondence between the NDBI and the LST gradually weakened over time.

Table 4. Pearson correlation coefficients between LST and NDBI for within-year and change-period analyses

| Analysis | Pearson r | p-value | Strength |
|---|---|---|---|
| **LST vs NDBI - 2013** | 0.743 | 0.003 | Strong |
| **LST vs NDBI - 2018** | 0.718 | 0.007 | Strong |
| **LST vs NDBI - 2024** | 0.694 | 0.011 | Strong |
| **LST vs NDBI - 2013 to 2018** | 0.312 | 0.027 | Moderate |
| **LST vs NDBI - 2013 to 2024** | 0.287 | 0.034 | Weak-Moderate |
| **LST vs NDBI - 2018 to 2024** | 0.261 | 0.041 | Weak-Moderate |

Source: Author's own elaboration based on Landsat 8 imagery

Within-year correlations were strong and significant across all three years. The highest value was recorded in 2013 ($r = 0.743$, $p = 0.003$), reflecting a tightly coupled spatial structure in which pixels with greater built-up intensity were reliably warmer than vegetated or water-covered areas. In the baseline year, the built-up core of GMC was relatively compact and spectrally distinct, producing a well-organised NDBI-LST pattern with minimal interference from mixed land cover at the urban periphery. The 2018 composite returned a slightly lower but still strong correlation of $r = 0.718$ ($p = 0.007$). Although absolute temperature values across GMC were lower in 2018, a consequence of inter-annual atmospheric variability during the November-December acquisition window. The spatial ordering of warmer built-up pixels over cooler non-built-up pixels was preserved. The modest decline in r relative to 2013 is partly attributable to the incremental expansion of built-up cover into peripheral zones during this five-year interval, which introduced transitional mixed pixels that somewhat diluted the structural clarity of the NDBI-LST relationship. By 2024, the within-year correlation had eased further to $r = 0.694$ ($p = 0.011$). Despite this decline, the value remained strong and crossed the 0.7 threshold, confirming that built-up surface intensity continued to be a reliable spatial predictor of elevated LST even as the city's land cover mosaic grew considerably more complex. The steady downward trend from 0.743 to 0.694 across the three years is best understood as a consequence of rapid peripheral expansion onto hilly and floodplain terrain, where new impervious surfaces are embedded within spectrally and thermally heterogeneous surroundings, rather than as evidence of any weakening in the urban heat penalty itself.

Change-period correlations between delta LST and delta NDBI were weaker than within-year values across all three temporal pairs, though all remained statistically significant. The 2013-2018 period yielded the strongest change-period value at $r = 0.312$ ($p = 0.027$), falling in the moderate range. This indicates a discernible but imperfect

tendency for pixels that gained built-up intensity to have also warmed over the five-year interval, with a substantial portion of inter-year thermal variability driven by atmospheric differences between the two acquisition windows rather than land cover dynamics alone. The 2013-2024 change period returned r = 0.287 (p = 0.034). Despite spanning the full eleven years of the study and capturing the largest cumulative built-up expansion, this value was weaker than the 2013-2018 estimate as a result of compounding atmospheric variability over a longer interval, combined with the topographically modulated thermal response of built-up expansion onto hillside terrain. The weakest change-period association was observed for 2018-2024, with r = 0.261 (p = 0.041), the period that also recorded the most rapid built-up growth, approximately 11.10 sq. km. The p-value of 0.041 sits closest to the 0.05 significance boundary among all six analyses, which is consistent with the inherently noisier nature of change-based correlations when inter-annual atmospheric variability between composites is not fully controlled.

Overall, the within-year r values of 0.694 to 0.743 establish that built-up surface intensity is a strong structural predictor of surface temperature within GMC, while the moderate-to-weak change-period values of 0.261 to 0.312 indicate that pixel-level thermal change over time is a multi-factor outcome in which surface cover conversion is one driver among several, alongside atmospheric variability, topographic aspect, and land cover heterogeneity at the urban fringe (Figure 6).

## Discussion

The results show that the built-up surface in Guwahati is always characterized by high land surface temperatures compared to non-urban land cover surrounding the city, which confirms the persistent thermal effects of urbanisation in the city (Borbora & Das, 2014). This trend is consistent with the reports of the rapidly growing cities in South and Southeast Asia, where the substitution of vegetated surfaces with impervious surfaces exacerbates the heating of the surfaces (Estoque et al., 2017; Weng et al., 2004). The temporal approach taken by the current study also demonstrates how the thermal properties of the urban environment change with the ongoing spatial expansion of the built-up landscape (Nath et al., 2021).

The slight decrease in the Pearson correlation coefficient between NDBI and LST from 2013 to 2024 should not be taken as evidence that the urban heat island effect is weakening. Zonal statistics give a more direct measure of thermal contrast and indicate that built-up areas were consistently warmer than non-built-up zones at any given time during the study period. Despite a slight decrease in the mean thermal difference that dropped to 1.76°C by 2024 compared to 1.98°C in 2013, the spatial extent of built-up land increased by about 65 percent. This means that the cumulative thermal exposure of the urban population must have risen even though the cumulative per-pixel temperature difference is likely to have stayed relatively constant (Arnfield, 2003; Santamouris, 2020).

The relatively low correlations found in the inter-period change analyses indicate that an important methodological point can be made concerning urban thermal studies. Numerous studies indicate a strong contemporaneous relationship between LST and built-up indices, and explain these as direct evidence of urbanisation-driven warming.

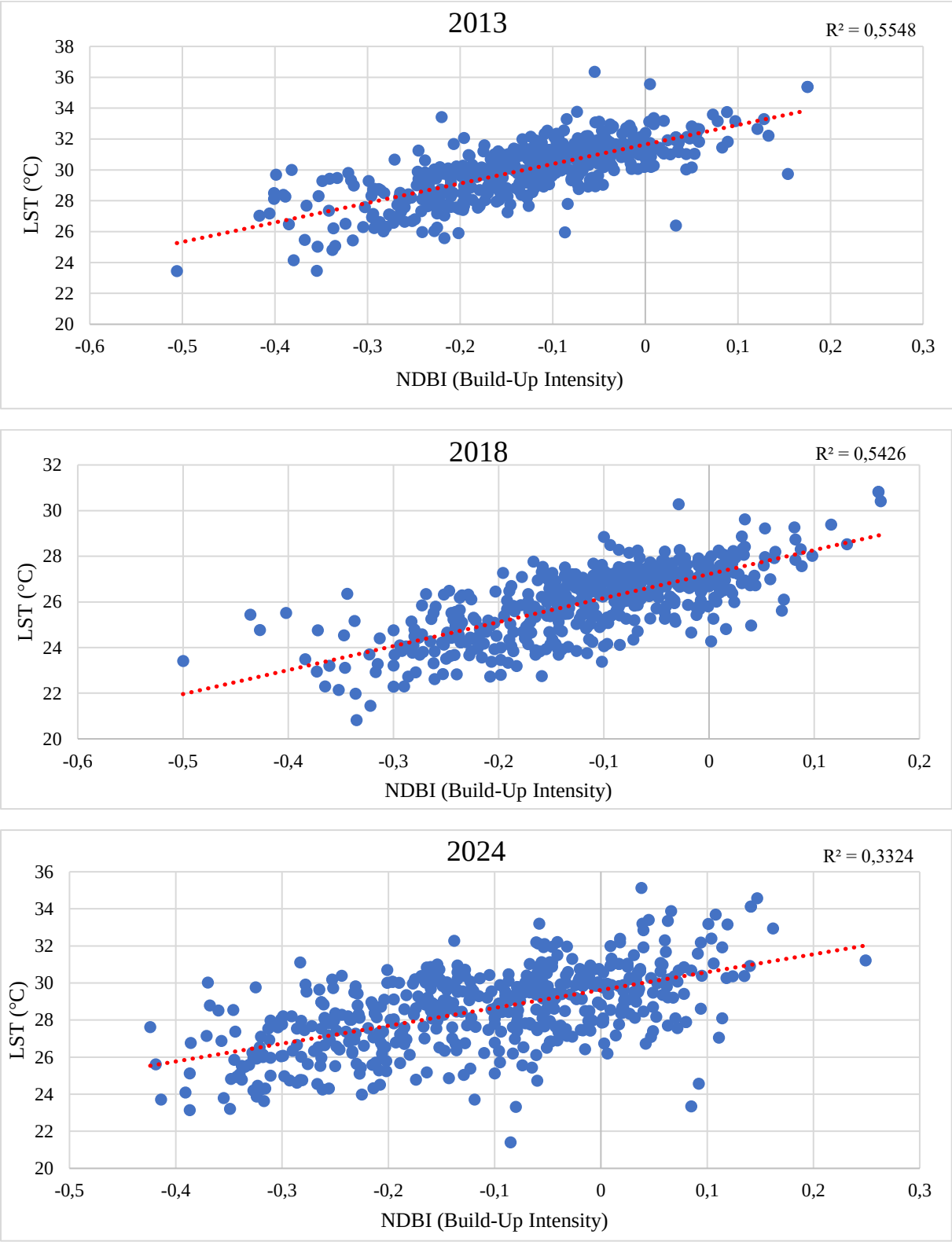


Figure 8. Scatterplots of LST versus NDBI for 2013, 2018, and 2024, with linear trend lines and R-squared values
Source: Author's own elaboration based on Landsat 8 imagery

But within-year associations are primarily evidence that urban surfaces are warmer than non-urban surfaces at a point in time and may in part be due to long-term structural land cover differences. Change-detection analysis provides a stricter evaluation since the former investigates whether those locations experiencing urban growth also experience a quantifiable warming over time (Deilami et al., 2018). The relatively low relationships between the change in NDBI and the change in LST in the GMC area show that additional environmental controls beyond built-up growth alone may influence the inter-annual thermal variability. It is likely that variations in atmospheric conditions, vegetation dynamics at a spatial scale, and topography contribute substantially to the variability in pixel-level thermal responses.

This spatial heterogeneity is further added to by the topography of Guwahati, which is very complex. Urban growth and development are increasingly extending onto the hill slopes around the city, thereby altering local surface energy balance conditions through elevation, slope orientation, and solar exposure. To illustrate, the south-facing slopes normally experience a higher solar radiation when compared to the north-facing slopes under the same land cover conditions. Consequently, the same increases in built-up intensity can have a variety of thermal responses depending on the topographic setting. This variability caused by topography may undermine statistical relationships between NDBI change and LST change without weakening the more general thermal impacts of urbanisation.

There are also some limitations in terms of methodology related to the NDBI-based urban extraction, which should be mentioned. In peri-urban areas, bare agricultural fields, bare sediments, and bare floodplain surfaces can produce positive NDBI values comparable to those of impervious urban materials at the 30 m spatial resolution of Landsat (He et al., 2010; Zha et al., 2003). Since there is a certain amount of agricultural land along the northern margins of GMC, it is likely that there will be some degree of commission error in the built-up classification. That can result in overestimation of the built-up extent and biased reduction of the observed thermal difference between urban and non-urban classes by the inclusion of relatively cooler non-impervious surfaces in the built-up category. Notably, such a bias would tend to underestimate, as opposed to overestimate, the measured thermal difference, which would, in turn, be a conservative estimate of the actual thermal impact of impervious urban surfaces.

The emissivity correction procedure followed in this study, based on NDVI-derived vegetation proportions, also comes with its fair share of uncertainty (Sobrino et al., 2004; Valor, 1996). The emissivity values are clustered around 0.986 in densely urbanised pixels with low vegetation cover, whereas heavily vegetated pixels are clustered around 0.990. Since this range of emissivities is relatively small, the correction has a limited effect in spectrally homogeneous urban or forested regions. Its impact is more evident in mixed pixels along the urban-vegetation transition zone, where NDBI values tend to be very near the classification threshold. Possible uncertainty in emissivity estimation in these transitional regions can thus contribute to some of the dispersion in the LST-NDBI relationship.

## Conclusions

This study tracked the relationship between urban built-up expansion and land surface temperature in the Guwahati Municipal Corporation across three time points from 2013 to 2024 using Landsat 8 imagery processed in Google Earth Engine. Built-up area grew from 24.33 sq km to 40.12 sq km over the study period, a 65 percent expansion. LST was persistently higher in built-up zones than in non-built-up zones throughout, with a thermal differential ranging from 1.50 to 1.98 degrees Celsius. Within-year Pearson correlations between LST and NDBI were significant and strong to moderate-strong across all years, declining from r = 0.681 in 2013 to r = 0.536 in 2024. Change-period correlations were consistently weaker, indicating that inter-annual pixel-level thermal change is not tightly determined by NDBI change alone.

Findings imply that Guwahati is persistently and spatially large-scale in having a thermal contrast between impervious urban surfaces and non-built-up land covers. Nevertheless, the thermal effects of further urban growth cannot be dictated exclusively by the transformation of surface covers. Rather, these patterns of variations in temperatures are formed due to the overall effect of inter-annual atmospheric variability, complex topographic conditions, and heterogeneous land cover composition along the urban fringe. With the further growth of the city and especially along the hill slopes on the south side, the future thermal behaviour of the urban environment will more and more depend upon the degree to which the new development will alter the existing vegetation cover and the manner in which the urban planning strategies will regulate the density, spatial distribution, and material composition of the growing built-up areas.

Further studies would enhance the validity of urban thermal assessment by including higher-resolution land-cover information, which can distinguish between impervious surfaces and spectrally similar bare agricultural or sediment-covered areas. Such ancillary data sets as night-time light images or building footprint data could further hone the definition of urban extent. Moreover, applying multiple Landsat scenes to each study year, along with seasonal stratification of observations, would provide a more robust framework for isolating atmospheric variability and land-cover-induced thermal change and would help strengthen the interpretation of long-term urban temperature dynamics.

## Funding

This research received no specific grant from any funding agency in the public, commercial, or not-for-profit sectors.

## Declaration of Competing Interests

The authors declare that they have no known competing financial interests or personal relationships that could have appeared to influence the work reported in this paper.

## Data Availability

This study used publicly available remote sensing and geospatial datasets accessed through Google Earth Engine. The datasets used are owned by their respective providers and are subject to their access terms. No new data were created during this study, and any derived results can be obtained from the corresponding author upon reasonable request

## Use of Generative AI and AI-Assisted Technologies

No generative AI or AI-assisted technologies were employed in the preparation of this manuscript.

## Acknowledgements

We take this opportunity to express our gratitude to the Department of Coastal Disaster Management, Pondicherry University, for providing us with the necessary support to complete this research.

## References

Arnfield A.J. (2003). Two decades of urban climate research: a review of turbulence, exchanges of energy and water, and the urban heat island. International Journal of Climatology, 23(1), 1–26. https://doi.org/10.1002/joc.859.

Bhattacharjee J., Mishra S., Acharjee S. (2022). Monitoring of land use/land cover changes and its implications in the peri-urban areas using multi-temporal landsat satellite data: a case study of Guwahati city, Assam, India. Proceedings of the Indian National Science Academy, 88(4), 778–789. https://doi.org/10.1007/s43538-022-00130-0.

Borbora J., Das A.K. (2014). Summertime Urban Heat Island study for Guwahati City, India. Sustainable Cities and Society, 11, 61–66. https://doi.org/10.1016/j.scs.2013.12.001.

Choudhury U., Singh S.K., Kumar A., Meraj G., Kumar P., Kanga, S. (2023). Assessing Land Use/Land Cover Changes and Urban Heat Island Intensification: A Case Study of Kamrup Metropolitan District, Northeast India (2000–2032). Earth, 4(3), 503–521. https://doi.org/10.3390/earth4030026.

Deilami K., Kamruzzaman Md., Liu Y. (2018). Urban heat island effect: A systematic review of spatio-temporal factors, data, methods, and mitigation measures. International Journal of Applied Earth Observation and Geoinformation, 67, 30–42. https://doi.org/10.1016/j.jag.2017.12.009.

Estoque R.C., Murayama Y., Myint S.W. (2017). Effects of landscape composition and pattern on land surface temperature: An urban heat island study in the megacities of Southeast Asia. Science of The Total Environment, 577, 349–359. https://doi.org/10.1016/j.scitotenv.2016.10.195.

Gorelick N., Hancher M., Dixon M., Ilyushchenko S., Thau D., Moore R. (2017). Google Earth Engine: Planetary-scale geospatial analysis for everyone. Remote Sensing of Environment, 202, 18–27. https://doi.org/10.1016/j.rse.2017.06.031.

Guha S., Govil H., Dey A., Gill N. (2018). Analytical study of land surface temperature with NDVI and NDBI using Landsat 8 OLI and TIRS data in Florence and Naples city, Italy. European Journal of Remote Sensing, 51(1), 667–678. https://doi.org/10.1080/22797254.2018.1474494.

He C., Shi P., Xie D., Zhao Y. (2010). Improving the normalized difference built-up index to map urban built-up areas using a semiautomatic segmentation approach. Remote Sensing Letters, 1(4), 213–221. https://doi.org/10.1080/01431161.2010.481681.

Nath B., Ni-Meister W., Choudhury R. (2021). Impact of urbanization on land use and land cover change in Guwahati city, India and its implication on declining groundwater level. Groundwater for Sustainable Development, 12. https://doi.org/10.1016/j.gsd.2020.100500.

Oke T.R. (1982). The energetic basis of the urban heat island. Quarterly Journal of the Royal Meteorological Society, 108(455), 1–24. https://doi.org/10.1002/qj.49710845502.

Parastatidis D., Mitraka Z., Chrysoulakis N., Abrams M. (2017). Online Global Land Surface Temperature Estimation from Landsat. Remote Sensing, 9(12). https://doi.org/10.3390/rs9121208.

Roy D.P., Wulder M.A., Loveland T.R., C.E. W., Allen R.G., Anderson M.C., Helder D., Irons J.R., Johnson D.M., Kennedy R., Scambos T.A., Schaaf C.B., Schott J.R., Sheng Y., Vermote E.F., Belward A.S., Bindschadler R., Cohen W.B., Gao F., … Zhu Z. (2014). Landsat-8: Science and product vision for terrestrial global change research. Remote Sensing of Environment, 145, 154–172. https://doi.org/10.1016/j.rse.2014.02.001.

Santamouris M. (2020). Recent progress on urban overheating and heat island research. Integrated assessment of the energy, environmental, vulnerability and health impact. Synergies with the global climate change. Energy and Buildings, 207. https://doi.org/10.1016/j.enbuild.2019.109482.

Sobrino J.A., Jiménez-Muñoz J.C., Paolini L. (2004). Land surface temperature retrieval from LANDSAT TM 5. Remote Sensing of Environment, 90(4), 434–440. https://doi.org/10.1016/j.rse.2004.02.003.

Sultana S., Satyanarayana A.N.V. (2020). Assessment of urbanisation and urban heat island intensities using landsat imageries during 2000–2018 over a sub-tropical Indian City. Sustainable Cities and Society, 52. https://doi.org/10.1016/j.scs.2019.101846.

Valor E. (1996). Mapping land surface emissivity from NDVI: Application to European, African, and South American areas. Remote Sensing of Environment, 57(3), 167–184. https://doi.org/10.1016/0034-4257(96)00039-9.

Voogt J.A., Oke T.R. (2003). Thermal remote sensing of urban climates. Remote Sensing of Environment, 86(3), 370–384. https://doi.org/10.1016/S0034-4257(03)00079-8.

Weng Q., Lu D., Schubring J. (2004). Estimation of land surface temperature–vegetation abundance relationship for urban heat island studies. Remote Sensing of Environment, 89(4), 467–483. https://doi.org/10.1016/j.rse.2003.11.005.

Zha Y., Gao J., Ni S. (2003). Use of normalized difference built-up index in automatically mapping urban areas from TM imagery. International Journal of Remote Sensing, 24(3), 583–594. https://doi.org/10.1080/01431160304987.